A robust and engineerable self-assembling protein template for the synthesis and patterning of ordered nanoparticle arrays

R. Andrew McMillan,* Jeanie Howard, Nestor J. Zaluzec, Hiromi K. Kagawa, Yi-Fen Li, Chad D. Paavola, and Jonathan D. Trent

NASA Ames Research Center, SETI Institute and Argonne National Laboratory

We report here a general technique for patterning nanoparticle (NP) arrays using a genetically engineered crystalline protein template to direct constrained chemical synthesis. The heat shock protein TF55β spontaneously assembles into an octadecameric double-ring cage structure called a chaperonin,[1] which in turn readily assembles into two-dimensional (2D) crystalline arrays.[2] We genetically removed a loop on TF55β that occludes the central pore of the assembled chaperonin and added a poly-Histidine (His$_{10}$) sequence to its N-terminus. With these modifications, the cores of assembled chaperonins possess 180 additional solvent accessible His residues, creating a region with enhanced affinity for metal ions that is spatially constrained by the interior dimensions of the chaperonin. When charged with Pd^{II}, the core the chaperonin becomes a site for selectively initiating the chemical reduction of magnetic transition metal ions (either Ni^{2+} or Co^{2+}) from precursor salts. This procedure yields arrays of bimetallic Ni-Pd or Co-Pd nanoparticles with dimensions defined by the chaperonin. Furthermore, the periodicity of the crystalline template imparts long range order to the patterned arrays that extends across the 2D protein crystal. Target applications of patterned arrays of transition metal NPs formed using this technique are high-density data storage media or for catalyzing the growth of arrays of materials such as nanotubes.

We previously demonstrated that self-assembling chaperonins modified with simple point mutations could be used to organize gold nanoparticles and semiconductor quantum dots.[3] Here we introduce an alternative strategy whereby we engineered the structure of TF55β to enhance the solvent accessibility of the chaperonin core and attached a peptide to the N-terminus, which is positioned within the core of assembled chaperonins, to add functionality to the template. Nucleation and constrained *in situ* chemical synthesis of alloyed metal NPs is selective to the functionalized chaperonins. The dimensions of the chaperonin cavities determine NP geometry, and the chaperonin 2D crystal lattice structure imparts long-range order and simultaneously patterns the NPs into arrays. The results from this templating approach demonstrate the general utility of engineering chaperonins to pattern materials, which now makes accessible the numerous peptide sequences identified by PCR-based and phage, cell surface and flagellar display screening techniques that can recognize, bind and in some cases even direct the synthesis of nanomaterials with preferred crystallographic orientation.[4]

We chose the 3d-4d binary alloy Ni-Pd as a target material because protocols for solution synthesis by electroless deposition, where borane-reduction of Ni is initiated by Pd, have been demonstrated.[5] Furthermore, bulk Ni-Pd alloys, which are ferromagnetic even at low concentrations of Ni, are promising candidates for use in magnetic data storage media.[6] The mismatch in atomic size of Pd vs Ni induces lattice strain, and thin films of
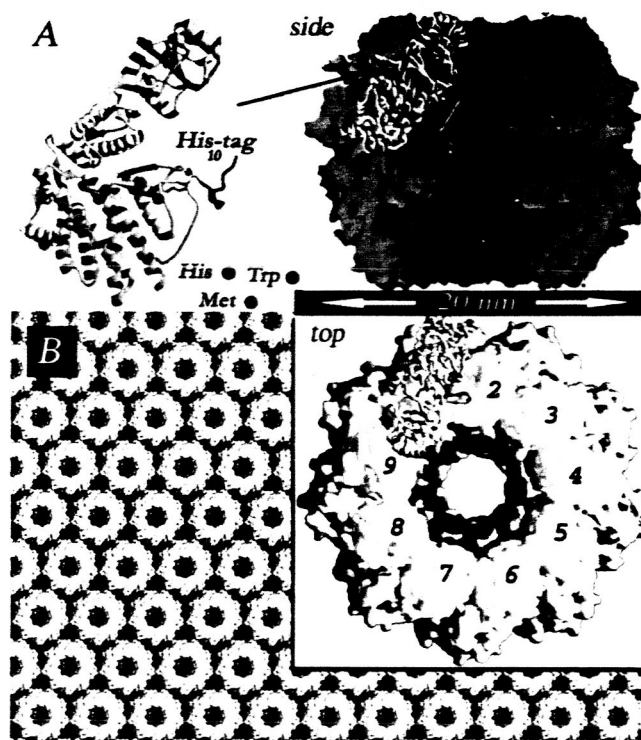

Figure 1. Assembly of engineered chaperonin templates (A) Subunit structure and views of assembled chaperonin cage structure highlighting residues likely involved in soft metal binding. (B) Hexagonal packing of chaperonins into 2D arrays.

Ni$_x$Pd$_{1-x}$ epitaxially grown on Cu substrates exhibit an *inverse spin reorientation transition (iSRT)* that could be exploited in novel high density data storage media.[7] Alternative targets accessible using our technique are the 3d-5d ferromagnetic nanomaterials CoPt and FePt which, in the chemically ordered (fct) $L1_0$ phase, exhibit high coercivity and magnetic anisotropy, and NPs smaller than 10 nm in diameter are potential candidates for use in high-density data storage media.[8]

The chaperonin protein TF55β was originally cloned from a hyperthermophilic organism which thrives at 85°C and pH 1-2. These robust proteins, even when mutated, tolerate a variety of modifications without losing their ability to self-assemble. This includes both the subunit self-assembly into chaperonins *and* the chaperonin self-assembly into 2D crystals that we exploit as templates (Figure 1). To functionalize the crystalline chaperonin templates we used structure-based protein design to guide the genetic engineering. We genetically removed a 32 amino acid loop from the subunit that, when assembled, occluded the symmetrical pores leading into the hollow core of the chaperonin

ABSTRACT

Self-assembling biomolecules that form highly ordered structures have attracted interest as potential alternatives to conventional lithographic processes for patterning materials. Here we introduce a general technique for patterning materials on the nanoscale using genetically modified protein cage structures called chaperonins that self-assemble into crystalline templates. Constrained chemical synthesis of transition metal nanoparticles is specific to templates genetically functionalized with poly-Histidine sequences. These arrays of materials are ordered because the template-driven synthesis is constrained by the nanoscale structure of the crystallized protein. This system may be easily adapted to pattern a variety of materials given the rapidly growing list of peptide sequences selected by screening for specificity for inorganic materials.

cages (Figure 1A). We further mutated this subunit by attaching a His_{10} sequence to the N-terminus, which is positioned within the core. When these subunits assemble into chaperonins (two opposed, symmetrical nine-subunit rings), they produce a cage structure 20 nm in diameter with a solvent accessible core containing up to 180 (10 per subunit) imidazole groups from the His_{10} peptides (Figure 1B). When assembled into hexagonally packed 2D crystals, the cores of the His-containing chaperonins are uniformly distributed in a periodic lattice (p312) and serve as the nucleation sites for constrained chemical synthesis of transition metal NPs (Figure 1C).

The chemistry we employed was adapted from established methods for electroless plating of coinage metals using Pt or Pd to initiate the reduction of precursor metal salt solutions. Briefly, to activate the His residues a preparation of chaperonin crystals (pH 7.5 in 25mM HEPES) was incubated with aqueous palladium(II) acetate (to 5 mM) and then dialyzed against a slightly acidic buffer (25 mM MES, pH 6.0). Palladium(II) is a soft metal ion and should tightly bind to the His-imidazole side groups (N-donors) at neutral to basic pHs, as well as to accessible tryptophans (N-donor) and methionines (S-donor) native to TF55β (Figure 1).

Washing the templates reduces background such as $[PdCl_4]^{2-}$ bound through electrostatic interactions with surface accessible charged groups such as amines (e.g. from Lys or Arg), which are protonated and do not act as N-donors. TEM analyses of washed templates reveal a periodic distribution of electron density indicating Pd concentrates in the hexagonally packed chaperonins, with a low comparable background (supporting information). For quantitative HR-TEM analysis, the arrays were prepared on either micromachined Carbon (Quantifoil) or etched SiN windows.
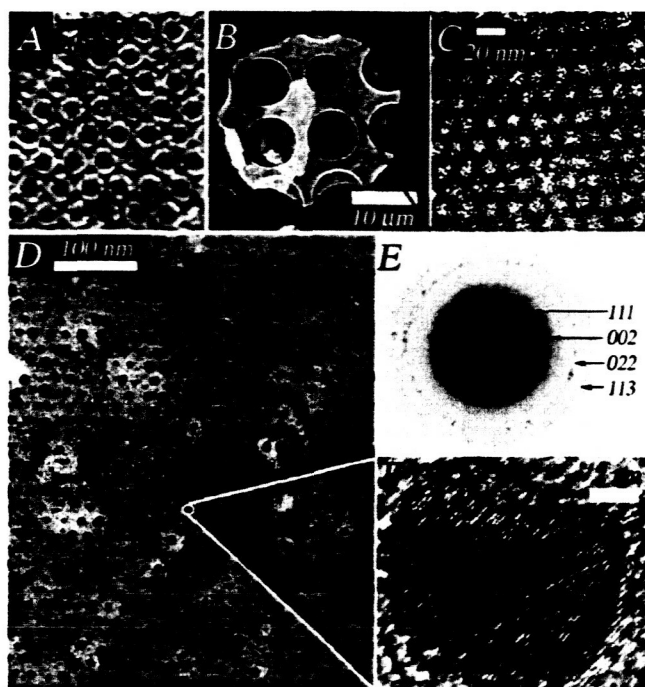

Figure 2. TEM imaging of Ni-Pd nanoarrays (A) Negatively stained hexagonally packed 2D chaperonin crystal (B) Low-mag HAADF-STEM image of templated Ni-Pd array on Quantifoil. (C) High-mag of area in (B) reveals clusters of 2-4 nm NPs form in the template pores and assume the hexagonal arrangement. (D) Low-mag bright-field TEM (60 kV) after coalescence of (C) into 8-10 nm NPs. (E) SAED pattern indexes to fcc and (F) HRTEM lattice imaging reveals single crystalline NPs.

Rinsed templates were applied to the substrates and perfused with a solution containing 1g/L dimethylamine borane-complex (DMAB) and either 1mM $NiSO_4$ or 1mM $CoSO_4$. Reduction of Ni^{2+} or Co^{2+} by DMAB requires initiation by Pd^0 (Figure 2A&B). Initial TEM imaging at 200 kV reveals clusters of 2-4 nm diameter NPs form within the cores of the crystallized chaperonin templates. Energy filtered (EF)-TEM maps of the abundance of Carbon in the arrays reveal the thin templates possess regions of monolayer thickness and a distribution of Nickel that confirms preferential accumulation to the central regions of the chaperonins (supporting information).

While imaging the arrays at low accelerating voltage (60 kV) we observed an electron beam interaction that coalesces the clusters of smaller NPs into larger NPs 8-10 nm in diameter (Figure 2D). This effect, which has been reported for palladium(II) acetate,[9] did not occur at 200 kV and was reproduced by heating samples at 500°C for 5 hrs either *in vacuo* or under an inert gas. The coalesced arrays of larger NPs maintain the periodic distribution across the template that is representative of the spacing defined by the lattice; although, some distortion of the long-range order was observed due to deterioration of the thin organic template under processing conditions.

Selected area electron diffraction (SAED) patterns confirm the larger annealed NP arrays index to (fcc). HR-TEM lattice imaging reveals a 2.03 +- 0.03Å lattice spacing for the crystalline NPs, which is consistent with the {111} d-spacing of Ni. X-ray analysis of the arrays confirms bimetallic composition; however, residual boron, which is known to form interstitial solid solutions with transition metals, was not quantified.

Our template-directed approach to NP synthesis addresses the challenge of substrate patterning because TF55β variants form extended, ordered, two-dimensional crystals 100 microns or more in diameter in solution. The dimensions of the annealed NPs are defined by the pore size of the chaperonins and their distribution in arrays is defined by the crystallinity of the template. Investigations into both the magnetic and catalytic properties of these transition metal nanoarrays are underway.

Supporting Information Available: Detailed procedures for synthesis and characterization of bimetallic NP arrays.

References:

(1) Trent, J. D.; Nimmesgern, E.; Wall, J. S.; Hartl, F. U.; Horwich, A. L. *Nature* 1991, 354, 490-3.
(2) Koeck, P. J.; Kagawa, H. K.; Ellis, M. J.; Hebert, H.; Trent, J. D. *Biochim Biophys Acta* 1998, 1429, (1), 40-4.
(3) McMillan, R. A.; Paavola, C. D.; Howard, J.; Chan, S. L.; Zaluzec, N. J.; Trent, J. D. *Nat Mater* 2002, 1, (4), 247-52.
(4) Brown, S. *Nat Biotechnol* 1997, 15, (3), 269-72. (b) Naik, R. R.; Jones, S. E.; Murray, C. J.; McAuliffe, J. C.; Vaia, R. A.; Stone, M. O. *Adv. Funcl. Mater.* 2004, 14, (1), 25-30. (c) Whaley, S. R.; English, D. S.; Hu, E. L.; Barbara, P., F.; Belcher, A. M. *Nature* 2000, 405, 665-668.
(5) (a) Brenner, A.; Riddell, G. E., *Proc. Am. Electroplaters Soc.* 1947, 34, 156. (b) Kirsch, R.; Mertig, M.; Pompe, W.; Wahl, R.; Sadowski, G.; Bohm, K.-J.; Unger, E. *Thin Solid Films* 1997, 305, 248-253.
(6) (a) Taylor, J. W.; Duffy, J. A.; Poulter, J.; Bebb, A. M.; Cooper, M. J.; McCarthy, J. E.; Timms, D. N.; Staunton, J. B.; Itoh, F.; Sakurai, H.; Ahuja, B. L. *Phys. Rev. B* 2001, 65, 024442. (b) Seider, M.; Kaltofen, R.; Muschiol, U.; Lin, M.-T.; Schneider, C. M. *J. Appl. Phys.* 2000, 87, (9), 5762.
(7) (a) Muschiol, U.; Seider, M.; Schneider, C. M.; Lin, M.-T. *J. Appl. Phys.* 2001, 89, (11), 6892-6894. (b) Matthes, F.; Seider, M.; Schneider, C. M. *J. Appl. Phys.* 2002, 91, (10), 8144-8146.
(8) (a) Sun, S.; Murray, C. B.; Weller, D.; Folks, L.; Moser, A. *Science* 2000, 287, 1989-1992. (b) Baglin, J. E. E.; Folks, L.; Kellock, A. J.; Terris, B. D.; Weller, D. K. U.S. Patent 6 331 364, 2001.
(9) Dieluweit, S.; Pum, D.; Sleytr, U. B. *Supram. Science* 1998, 5, 15-19. (b) Stark, T. J.; Mayer, T. M.; Griffis, D. P.; Russell, P. E. *J. Vac. Sci. Tech.* 1991, 9, (6), 3475-3478.

Supporting Information:

Procedure for synthesis of bimetallic nanoarrays: Two-dimensional crystals of the engineered chaperonin were prepared at a protein concentration of 1 mg/mL as described elsewhere. To charge the crystals with the noble metal, 10 microliters of 100mM Palladium(II) Acetate was added to 100 microliters of 2D crystal slurry. After incubation at room temperature for one hour, excess Pd was rinsed from the crystallization suspension by microdialysis against 25 mM MES buffer, pH 6.0 overnight followed by 2 hr against DDI-H_2O. The Pd-charged crystals were applied to either carbon stabilized formvar TEM grids or micromachined carbon ("Quantifoil") substrates and floated onto 100 microliters of a mixture of either 1mM Co SO_4 or 1 mM Ni SO_4 and 1g/L Dimethylamino Borane complex (DMAB) for 1 minute. Samples were washed with DDI-H_2O and dried *in vacuo* prior to analysis.
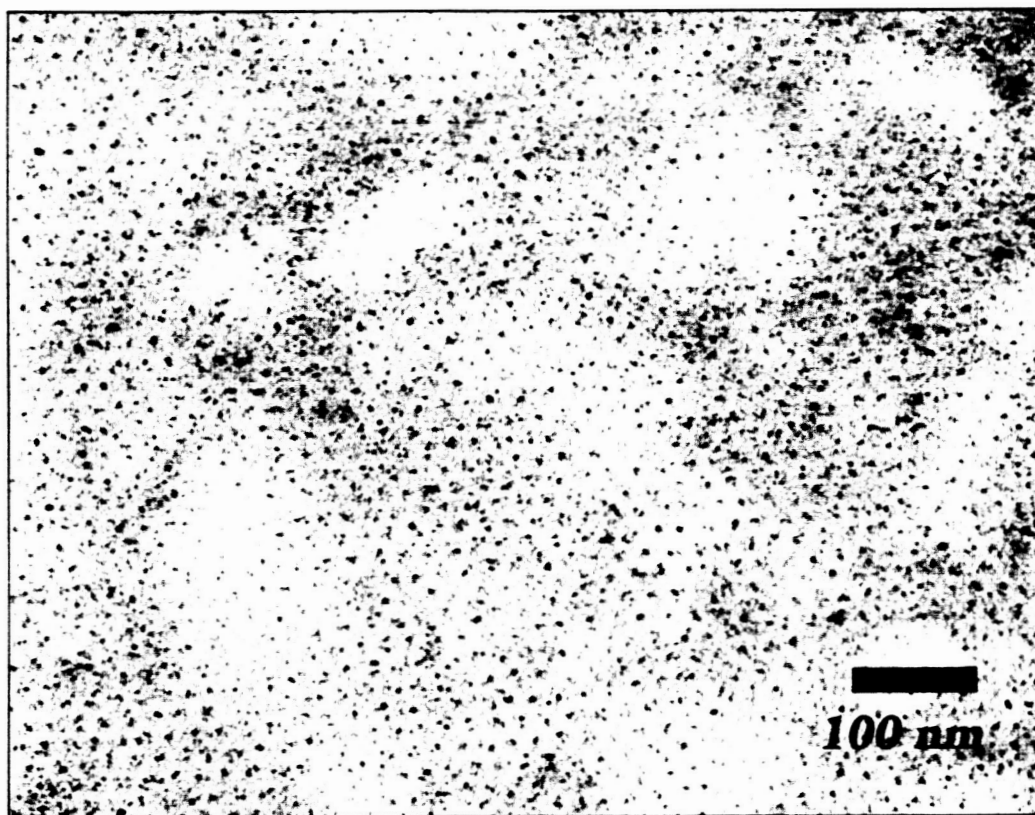

Figure S1. Conventional TEM image (60 kV) of Pd-charged template after rinsing by dialysis. The periodicity of the electron density is indicative of Pd centrally accumulated in engineered chaperonins hexagonally packed in the 2D crystal. Control experiments using protein crystals without the His-10 modification did not possess any apparent periodicity in electron density when incubated with Pd solutions and washed.
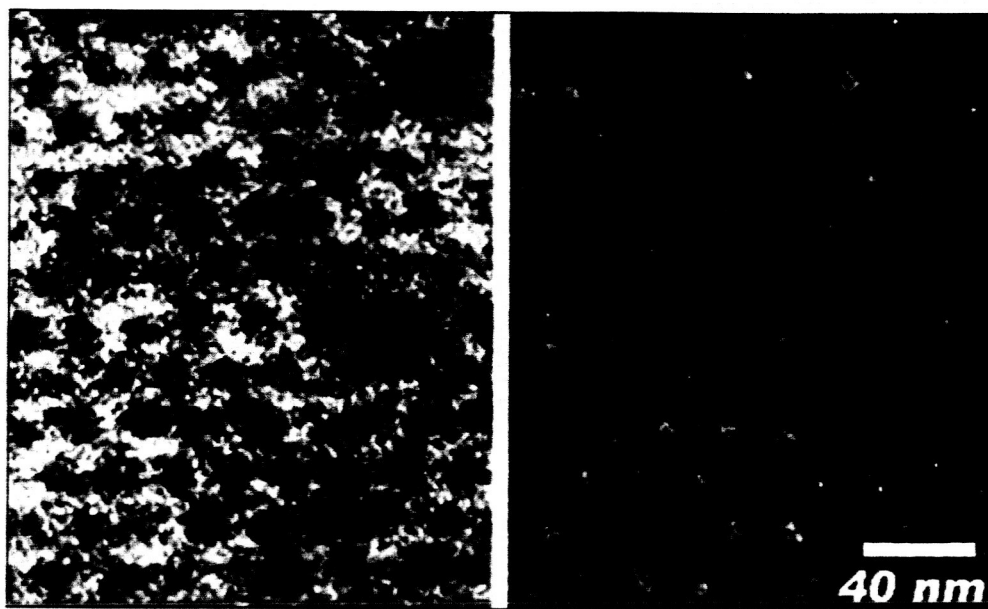
Figure S2. Elemental distribution imaging (EELS map) of Ni-Pd array prior to sample annealing from Figure 2 (B) and (C) collected on an area of the sample positioned over a hole in the substrate which enables accurate mapping of the distribution of different elements on the template. The left image was generated by filtering the loss signal (K edge) and mapping the carbon distribution while the image on the right maps Ni.
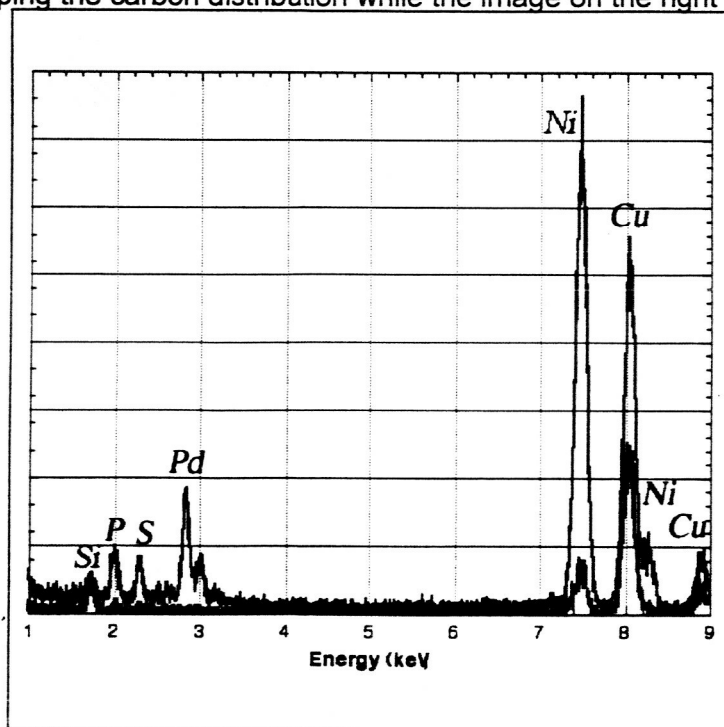

Figure S3. XEDS spectra collected from sample from **Figure 2** (B) and (C) from the text comparing Ni-Pd array suspended over the holes in the support film (blue trace) and background on the carbon support film (red trace).
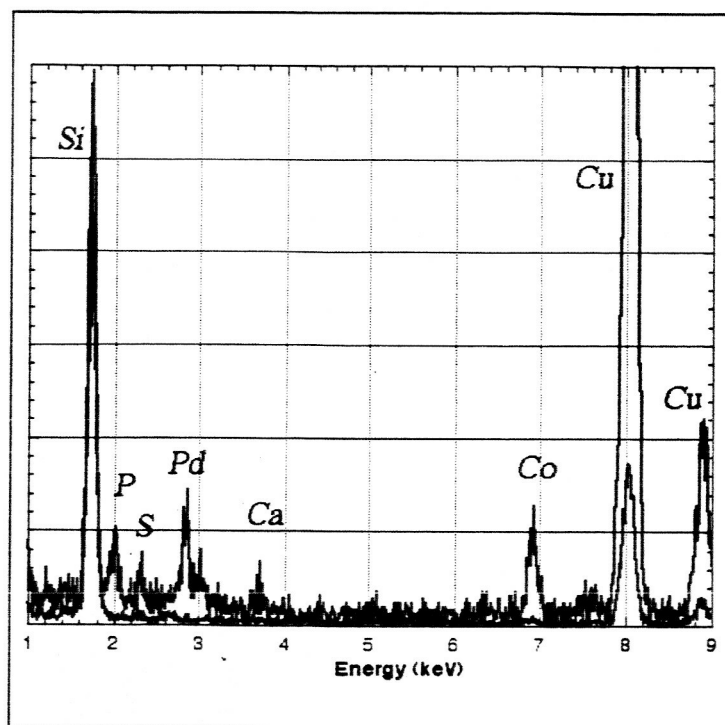
Figure S4. XEDS spectra similar to Figure S2 collected from a Co-Pd array sample prepared on a SiN substrate confirming the presence of Co and Pd in the arrays.

Figure S5. HR-TEM lattice image of three coalesced Co-Pd nanoparticles (arrows) similar to that in **Figure 2F** from the text, but synthesized by substituting $CoSO_4$ for $NiSO_4$. The lattice spacing is 0.22 nm, which is consistent with the {111} d-spacing for fcc Co (2.15Å, JCPDS, #15-806).